Neurocomputing 496 (2022) 158–165

Contents lists available at ScienceDirect

Neurocomputing

journal homepage: www.elsevier.com/locate/neucom

Role of astrocytes in the self-repairing characteristics of analog neural networks

Negin Veisi [a], Gholamreza Karimi [a,*], Mahnaz Ranjbar [b], Derek Abbott [c]

[a] Department of Electrical Engineering, Faculty of Engineering, Razi University, Kermanshah 6714967346, Iran
[b] Young Researchers and Elite Club, Kermanshah Branch, Islamic Azad University, Kermanshah, Iran
[c] School of Electrical & Electronic Engineering, The University of Adelaide, SA 5005, Australia

ARTICLE INFO

Article history:
Received 2 June 2020
Revised 28 January 2021
Accepted 23 January 2022
Available online 29 January 2022

Keywords:
Neural network
Astrocyte
Self-repairing
Analog

ABSTRACT

Self-repair is fundamental to biological neural networks. In a neural network with a large number of elements, the probability of failure of each component increases. With the breakdown of each part, there may be a significant difference in the final results that will be completely affected by this defect. The existence of a process for detecting the error and compensating it by recruiting healthy elements leads to improved performance. This is where adjacent synapses proxy faulty synapses to avoid disturbances in the network function, thereby compensating the incurred error. In the present research, a self-repairing analog circuit is designed based on an astrocyte-neuron interaction and new synapse architecture. The designed circuit builds upon a software model of an astrocyte-neuron network with the proven ability to detect errors and undertake self-repair. The results obtained from our circuit show that, when an error occurs in the synapses associated with a neuron, the currents within functioning synapses of the same neuron increase. This increase is made by receiving feedback from adjacent astrocytes and other synapses. The process maintains the network function, compensating incurred errors in the network, presenting a neural network-based analog circuit with self-repairing capability, while considering the effect of astrocytes. In this paper, extensive simulation results using HSPICE with 0.35 μm CMOS technology are provided for the evaluation of the proposed circuit.

1. Introduction

The increasing use of neural networks in many applications has attracted the attention of many researchers in this field [1–4]. Neural networks comprise components such as neurons, synapses, astrocytes, etc. Different mathematical models and circuits are applied in each case [4–12]. The neuromorphic circuit is a new topic that combines medical and electrical engineering in recent decades [1–3,13,14]. To have an optimal hardware neural network circuit, we need to properly design these mathematical models so that we can best implement neural networks. So far, different analog and digital circuits are presented for neurons, synapses, and astrocytes. Different components of nervous systems play various roles to ensure correct function [5,6].

Self-repair is the method that assists biologically-inspired nervous systems to compensate for the task of faulty synapses.

The astrocyte plays a key role in the interaction between components of neural networks [1,7–15]. Astrocytes, in addition to feeding on different parts of the nervous system, play an active role in the functions of information transfer, learning and etc. [1,4,16,17].

In real neural networks, when network components have a problem, other components detect it and fix it approximately. In this condition, the neighbor synapses and neurons compensate for the incurred faults. The astrocyte is one of the components that helps the synapses to compensate for these faults.

One of the tasks recently discovered by researchers is the role of astrocytes in the self-repair of neuronal networks [1,17,18]. Self-repair involves the cooperation of various parts of the neural network to compensate for faults. So far, there has been a significant number of studies in this area [1,3,14,17-20] that show the ability of the astrocyte to repair faults. One of the cases used is the control of robots using neural networks and self-repairing algorithms, which has been implemented digitally in [3]. Astrocytes, by having glutamate (Glu) at the output known as the e-SP signal, create a self-repairing network and compensate for any incurred faults. By applying astrocyte self-repairing rules, fault tolerance can be improved and the desired response is obtained. This signal is affected by the frequency of all neurons around the astrocyte,

* Corresponding author.
E-mail address: ghkarimi@razi.ac.ir (G. Karimi).

https://doi.org/10.1016/j.neucom.2022.01.077
0925-2312/

which due to its global signal can be less affected by errors in the network. This process causes a network fault due to a defect in the elements, does not affect the final output of this signal, and is a suitable flag for initiating self-repair.

The self-repair is used in all of the networks where the possibility of damaging network components is high and there is a need for repair and compensation.

In this paper, we present a new astrocyte-neuron analog circuit with self-repair capability, which is potentially a step forward in advancing analog neural networks. We use the astrocyte circuit [16] in a small neural network to show that it can generate a global signal (using the e-SP signal) as a feedback signal for repairing incurred faults in the neural network. So, the main contribution of the proposed approach is based on a new proposed biologically-inspired self-repair structure by using the astrocyte circuit, capturing the self-repairing capability of biological neural networks.

The rest of the paper is organized as follows: Section II, explains the self-repairing neural network model. The proposed circuit implementation of astrocyte mediated self-repair is described in Section III. The simulation results of the proposed circuit are presented in Section IV. Finally, in Section V, the importance and some future directions of the present research are discussed.

2. Self-repairing neural network model

As mentioned, the goal of this paper is to present a new astrocyte-neuron interaction analog circuit that captures the self-repairing behaviors of spiking neural networks.

Astrocytes can cover a large number of synapses connected to a neuron and connect to several neighboring neurons. These astrocytes have many receptors that are used for synaptic information transfer. For example, the astrocytes have connection points for endocannabinoids or 2-arachidonoylglycerol (2-AG). Endocannabinoids are retrograde messengers that are released in postsynaptic neuronal depolarization [21]. When an action potential reaches a presynaptic axon, neural transporter (glutamate) is released in the synaptic gap and binds to dendrite, resulting in postsynaptic neuronal depolarization and release of 2-AG. The released 2-AG may then reach the presynaptic terminal via either of two paths:

1) Direct: 2-AG binds directly to type 1 Cannabinoid (CB1Rs) receivers in the presynaptic terminal, resulting in reduced transmission probability of release (PR) that is referred to as Depolarization induced Suppression of Excitation (DSE) [21].
2) Indirect: In indirect mode, 2-AG binds to astrocyte CB1Rs and results in the release of Inositol trisphosphate (IP_3) that enhances the level of IP_3 in the astrocyte; this, in turn, actuates Ca^{2+}intra-cellular broadcast (ICB). An increased level of Ca^{2+} leads to an astrocytic broadcast of glutamate that binds to the presynaptic group I Metabotropic Glutamate receivers (mGluRs). This signaling increases PR, which is called e-SP [22].

The PR of each synapse is affected by DSE and e-SP, as described in the following [17,18]:

$$\mathrm{PR}(t) = \left(\frac{\mathrm{PR}(t_0)}{100} \times \mathrm{DSE}(t)\right) + \left(\frac{\mathrm{PR}(t_0)}{100} \times \mathrm{eSP}(t)\right) \tag{1}$$

where PR (t_0) is the initial value of PR for each synapse. In order to model the released 2-AG, it is assumed that each time the postsynaptic neuron makes a spike (fires), 2-AG is released and can be given by the following equation [14,17,18]:

$$\frac{d(\mathrm{AG})}{dt} = \frac{-\mathrm{AG}}{\tau_{\mathrm{AG}}} + r_{\mathrm{AG}}\delta(t - \mathrm{t_{sp}}) \tag{2}$$

where AG denotes the released amount of 2-AG, τ_{AG} and r_{AG} are decay and generation rates of 2-AG, respectively, and t_{sp} is the time of the postsynaptic spike. When 2-AG binds to the Cannabinoid CB1 receptors (CB1Rs) on the astrocyte, IP_3 is produced following a behavior similar to that described by the gatekeeper model [15] that depends on the released amount of 2-AG and is described by the following equation [14,17,18]:

$$\frac{d(\mathrm{IP_3})}{dt} = \frac{\mathrm{IP_3^*} - IP_3}{\tau_{\mathrm{IP_3}}} + r_{\mathrm{IP_3}}\mathrm{AG} \tag{3}$$

where IP_3 is the amount of exist in the cytoplasm. Here, IP_3^* is the basic amount of IP_3 when the cell is in steady state. $r_{AG,}$ r_{AG} are decay rate and production rate, respectively.

In this model, Li-Rinzel astrocyte model [23] is used as follows:

$$\frac{d(\mathrm{Ca^{2+}})}{dt} = J_{\mathrm{chan}}(\mathrm{Ca^{2+}}, h, \mathrm{IP_3}) + J_{\mathrm{leak}}(\mathrm{Ca^{2+}}) - J_{\mathrm{pump}}(\mathrm{Ca^{2+}}) \tag{4}$$

where J_{chan} is opening of Ca^{2+} broadcast by the mutual gating of Ca^{2+} and IP_3 concentrations, J_{pump} is pumped amount of Ca^{2+} from cytoplasm toward the endoplasmic reticulum (ER), J_{leak} is the amount of Ca^{2+} leaked from ER, and h is the activated fraction of inositol 1, 4, 5-trisphosphate receptors (IP3Rs). In this method, a linear relationship is assumed between the released 2-AG and DSE, as follows [17,18]:

$$\mathrm{DSE} = \mathrm{AG} \times K_{\mathrm{AG}} \tag{5}$$

where AG refers to the released amount of 2-AG by postsynaptic neuron (given by Equation (2)) and K_{AG} is a scaling factor for converting the level of 2-AG to the desired negative range. Intracellular dynamic astrocytic calcium uses astrocyte for adjusting the broadcast of glutamate. Target glutamate release (group I mGluRs) is given by the following equation [14,17,18]:

$$\frac{d(\mathrm{Glu})}{dt} = \frac{\mathrm{Glu}}{\tau_{\mathrm{Glu}}} + r_{\mathrm{Glu}}\delta(t - \mathrm{t_{Ca}}) \tag{6}$$

where Glu is the amount of glutamate, τ_{Glu} and r_{Glu} are decay and generation rates of glutamate, respectively, and t_{Ca} is Ca^{2+} threshold pass time.

The level of e-SP depends on the amount of glutamate, which is modeled by (7) where τ_{eSP} is the decay rate of e-SP and m_{eSP} is a weighting constant [14,17,18],

$$\tau_{\mathrm{eSP}}\frac{d(\mathrm{eSP})}{dt} = -\mathrm{eSP} + m_{\mathrm{eSP}}\mathrm{Glu}(t). \tag{7}$$

The adopted synapse model is a probability-based model wherein a uniform distributed pseudo-random number generator generates a random number between 0 and 1 whenever a presynaptic spike reaches the synapses. If the value of the generated random number is equal to or smaller than broadcast PR, an I_{inj} flow is injected to leaky integrate-and-fire neuron (LIF) [24] called I^i_{syn}, which can be expressed as the following equation [17,18]:

$$\mathrm{I}^i_{\mathrm{syn}} = \begin{cases} \mathrm{I_{inj}} & \text{random} \le \mathrm{PR} \\ 0 & \text{random} > \mathrm{PR} \end{cases} \quad i = 1, 2 \text{ number of neurons.} \tag{8}$$

The parameter values are list in Table 1.

3. Proposed self-repairing analog circuit

In this section, we begin by presenting the concept and principles of self-repairing on spiking astrocyte-neuron networks followed by delivering a detailed discussion on the proposed self-repairing analog circuit and its implementation.

Table 1
Parameter values of the self-repairing model.

Parameter	Value	Parameter	Value	Parameter	Value	Parameter	Value
$IP_3{}^*$	0.16 μM	τ_{Ca}	1 s	K_{AGx}	−4000	r_{Glu}	10 μMs^{-1}
r_{ip3}	0.5 μMs^{-1}	τ_{AG}	10 s	τ_{Glu}	100 ms	m_{eSP}	55 x 10^3
t_{ip3}	7 s	r_{AG}	0.8 μMs^{-1}	τ_{eSP}	40 ms		

3.1. Self-repairing strategy on spiking astrocyte-neuron networks

Fig. 1 describes the architecture of the proposed circuit that is composed of two neurons and one astrocyte. This small network is used to demonstrate principles of self-repair in hardware. In this model, each neuron is connected to several synapses. The main component of this network is the neuron facility (e.g. neurons 1 and 2 in Fig. 1). Inputs into neurons are signals from synapses, and output signals include a neural spike, 2-AG, and DSE. The neural model proposed by [8] was used in the neuron facility. When a postsynaptic neuron spikes, 2-AG is released according to Eq. (2) while DSE is produced according to Eq. (5) which is the main process in neuron facilities. The released 2-AG binds to CB1Rs on the astrocyte, indirectly increasing PR of synaptic transmission. Nevertheless, DSE imposes a direct impact at postsynaptic terminal, i.e. reduces PR of the synaptic transmission.

The second key component is the astrocyte facility. As shown in Fig. 1, the astrocyte facility receives 2-AG signal from the postsynaptic neuron and generates e-SP signal for the synapsis, which can enhance PR of synaptic transmission.

The third component of this network is the synapse facility. The synapse facility is designed using the probability-based synapse model as formulated in Eq. (8). The Synapse facility receives input presynaptic spikes and DSE/e-SP from neuron/astrocyte. It has an output signal (i.e. synapse out in Fig. 1) which is connected to the neuron facility. As discussed previously, synaptic transmission PR is set by DSE and e-SP. Two PR setters are designed to adjust the process, one of which (for DSE) tends to reduce the value of PR, with the other one (for e-SP) increasing the value of PR.

3.2. Self-repairing mechanism in analog circuit

The proposed analog circuit includes two neurons and one astrocyte, with each neuron being connected to 10 synapses. Each of these components is investigated in the following.

3.2.1. Neuron

The neural circuit used in the present paper was designed based on the numerical model presented by Izhikevich [9] that was designed by Wijecon [8]. This circuit includes 14 MOSFET transistors and has two state variables: membrane potential (V) and slow variable (U). Dynamics of the circuit is approximated using a series of equations [10]:

$$\frac{dV}{dt} = \begin{cases} a_1V^2 - a_2V - a_3U^2 + a_4U + a_5 + i_1 & \text{when } V > U - V_T \\ a_6V^2 - a_7V - a_8UV + i_2 & \text{otherwise} \end{cases} \tag{9}$$

$$\frac{dU}{dt} = a_9V^2 - a_{10}V - a_{11}U^2 + a_{12}U + a_{13} \tag{10}$$

If

$$V > V_{th} \text{ then } \begin{cases} V \leftarrow c \\ U \leftarrow U + d \end{cases} \tag{11}$$

where a_i, V_T, V_{th}, i_i, c, and d are constants which depend on the transistor dimensions (e.g. W/L), region of operating, bias voltages, and input current. This circuit generates a variety of cortical neuronal firing patterns [10,11]. This neural circuit has a compact layout and low power consumption in the range of 9 pJ/spike [12].

3.2.2. Astrocyte

Attachment of the released 2-AG from the dendrite to CB1Rs on the astrocyte releases some IP_3 into the cytoplasm of the astrocyte. These IP_3s bind to IP_3Rs on endoplasmic reticulum (ER) (ER is a long network of conduits and vesicles used for storing calcium in the cell [25]). The connection between IP_3 and IP_3Rs results in opening Ca^{2+} channels and Ca^{2+} broadcast for ER into the cytoplasm. The increase in Ca^{2+} results in the release of glutamate which returns to the synaptic gap and binds to presynaptic group I mGluRs receivers. This signaling enhances synaptic transmission probability and generates an e-SP signal which contributes to the self-repairing behavior of faulty synapses [14,17,18].

The used astrocyte circuit in the present research is based on the astrocyte dynamic model presented in [26]. Dynamics of the astrocyte model is described by the following system of differential equations:

$$\begin{cases} \dot{q} = (1 + \tanh k_1[Z - K_2])(1 - q) - k_3q \\ \dot{P} = -K_4p + K_5 + K_6q \end{cases} \tag{12}$$

where q is the internal state of astrocyte, k_i (i = 1, 2, …, 6) is constant (as listed in Table 2), and Z and p are the input and the output of the astrocyte, respectively.

Fig. 2 illustrates the general structure of the used astrocyte which has been reported in the previous work in detail [16].

As shown in [16], the used astrocyte circuit is based on the simplified model of astrocyte dynamics (formulated in Eq. (12)) and composed of two functional parts. Two modal variables (p, q) are presented using voltages of the capacitors C_p (V_p) and C_q (V_q), respectively. Indeed, the performance of the circuit is based on the charging and discharging behaviors of the capacitors C_p and C_q which generate p and q modes in the astrocyte dynamic model.

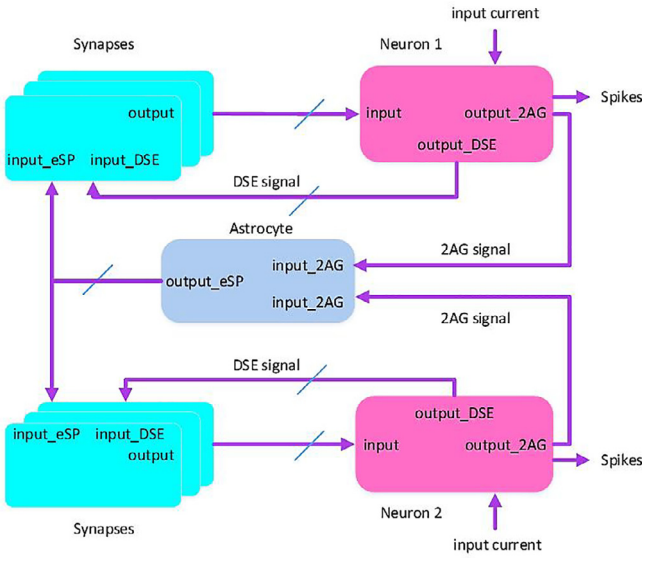

Fig. 1. Proposed block diagram architecture of an analog spiking astrocyte-neuron network for self-repairing mechanism.

Table 2
Parameter values of Astrocyte dynamic model [26].

Parameter	Value	Parameter	Value
k_1	1	k_2	2
k_3	2	k_4	1
k_5	0.05	k_6	1.5

The employed astrocyte circuit (Fig. 2) has been studied extensively, including equations governing the behavior of the circuit and its transistor-level design implementation as mentioned in the previous work [16].

3.2.3. Synapse

The architecture of the proposed synapse used in the proposed circuit is shown in Fig. 3. This includes two DPI (Differential Pair Integrator) circuits [6], one comparator, and one resistor. In this part of the circuit, on one hand, the neuron receives the value of e-SP which is a global value, and on the other hand, the value of DSE as a local measure is transmitted to the circuit by DPI synapse; finally, the circuit produces an appropriate current to be injected into the neuron.

Prior to injection into the neuron, the generated current is compared against random value by a comparator. If a suitable condition is established, the generated current output of the comparator is injected into the neuron. In fact, this random value determines the probability of healthiness of the synapse.

4. Simulation results

Presented in this section are the results of simulating the designed circuit. First, in order to demonstrate suitable properties of the astrocyte [16] for this particular circuit, simulation results were investigated for different input data at different frequencies. In this simulation, input pulses with various frequencies were applied to the astrocyte circuit and the output behavior of the astrocyte with changing the frequency was demonstrated. Results of this simulation are shown in Fig. 4. According to the results reported in [16] and Fig. 4, one of the characteristics of the astrocyte is its frequency adaptation that has improved performance at higher frequencies. These results show that when the input frequency of astrocyte is high, the output astrocyte produces a continuous signal. This continuous signal plays the role of the Glu signal in the neural network.

In the next experiment as shown in Fig. 5, an input sinusoidal waveform with a peak amplitude of 1.5 V is applied to the astrocyte circuit at different frequencies. As can be observed, the general shape and the qualitative behavior of trajectories are similar for the model and the developed circuit over a range of amplitudes.

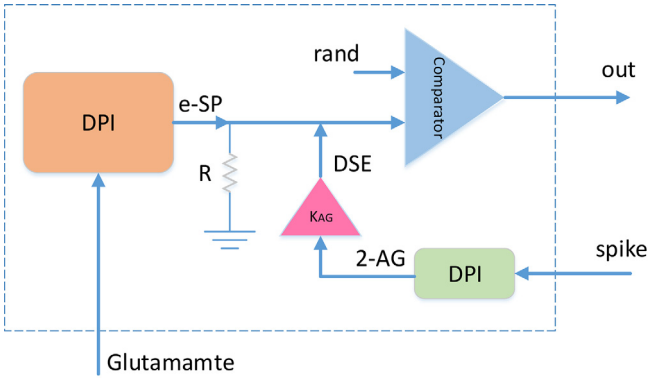

Fig. 3. Architecture of the proposed synapse used in the proposed self-repair circuit.

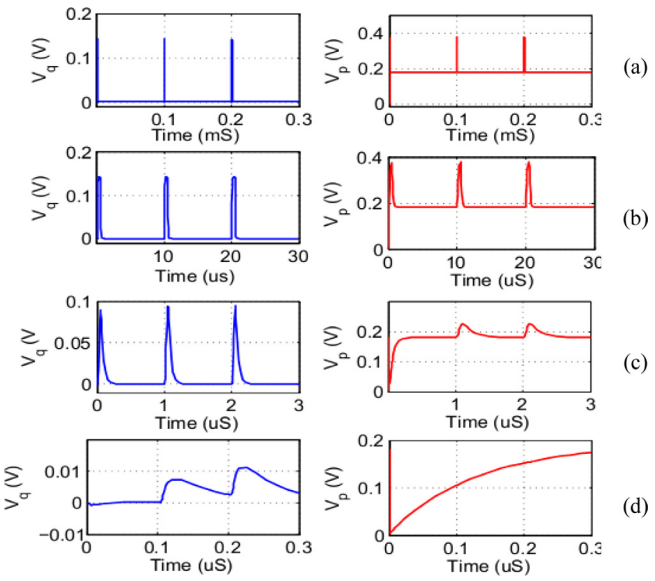

Fig. 4. Simulation results of astrocyte circuit for different input pulse frequencies with V_{Amp} = 1.5 V. (a) f = 10 kHz, (b) f = 100 kHz, (c) f = 1 MHz, (d) f = 10 MHz.

This characteristic, as seen in Fig. 4 and Fig. 5, significantly contributes to the self-repair mechanism. The root mean square error (RMSE) and percent of error between state variables of the astrocyte model in MATLAB simulations and output voltages of the astrocyte circuit in HSPICE simulations are listed in Table 3.

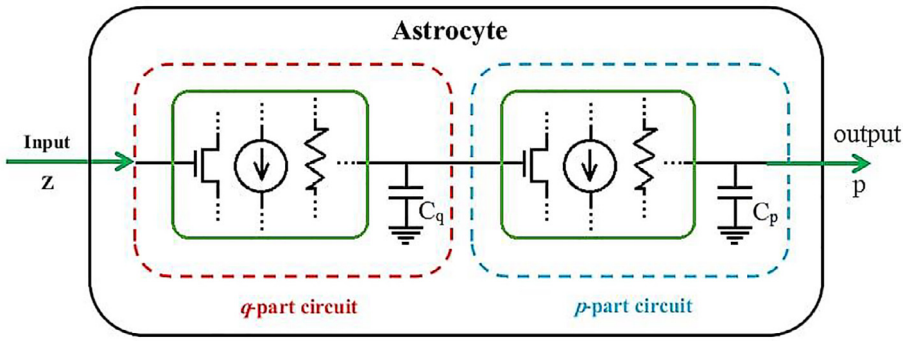

Fig. 2. Illustrative structure of the astrocyte circuit [16] used in this work.

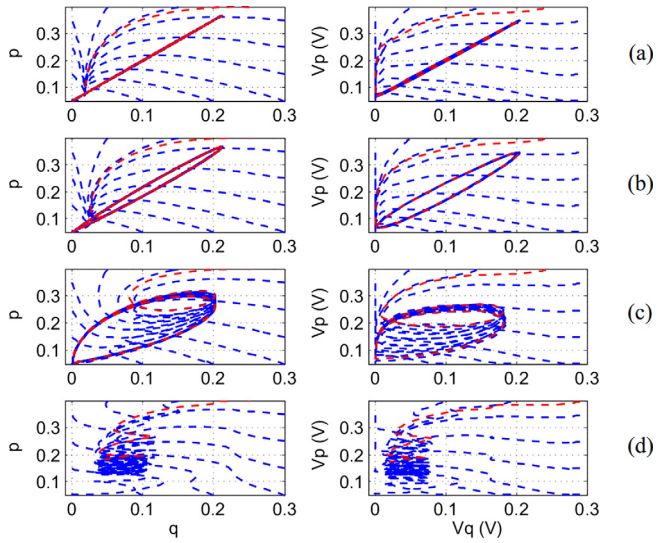

Fig. 5. The phase plane of both original model and the proposed analog astrocyte circuit with V_{Amp} = 1.5 V and (a) f = 10kHz, (b) f = 100kHz, (c) f = 1 MHz, and (d) f = 10 MHz. (Left panels) The results of the MATLAB simulations, (Right panels) The results of the HSPICE simulations.

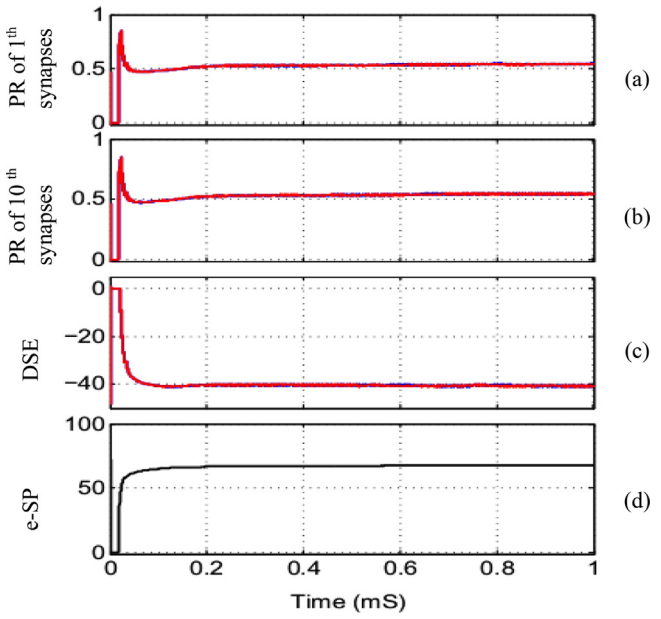

Fig. 6. Simulation results with 0% fault rate. (a) PR of the first synapses, (b) PR of the 10th synapses, (c) DSE signal of both neurons, (d) global e-SP signal. (red color) neuron #1, (blue color) neuron #2. (For interpretation of the references to color in this figure legend, the reader is referred to the web version of this article.)

These simulation results show sufficient accuracy of the astrocyte circuit for use in different circuits. By considering the changes in output astrocyte behavior at different frequencies, appropriate characteristics for self-repair can be found. As shown in this simulation, by increasing the input frequency of astrocyte, the astrocyte output signal has a continuous signal behavior. When the input frequency of astrocyte increases, the little change of input frequency cannot change the astrocyte output significantly. This property causes to keep constant of approximately e-SP signal in different faults.

In order to demonstrate this effect, the designed circuit was investigated and analyzed to show the appropriate influence of the astrocyte on the self-repairing behavior of the designed analog circuit. This circuit was simulated both in a healthy state and for different fault rates.

As mentioned in Section 2, Fig. 1 illustrates the self-repairing mechanism of an astrocyte-neuron network. This network consists of one astrocyte, two neurons, and 20 synapses (10 synapses per neuron), and each neuron has several synapse inputs. Fig. 3 shows the architecture of the proposed synapse used in the proposed self-repair circuit. When the neuron becomes active and spikes, the 2-AG and DSE signals are applied to the astrocyte and to the synapses associated with each neuron respectively. And astrocyte generates a global signal (e-SP) for all the synaptic terminals, modulating the transmission PRs of all synapses. This synaptic modulation is the key process for the self-repairing mechanism. So that, when some associated synapses of a neuron are faulty and cannot able to play their role in the network, adjacent synapses, by receiving feedback from neuron and astrocyte, partly compensate the roles of faulty synapses (causing to maintain the neuron average firing rate through redistribution of PRs across all the synapses), having the self-repairing capability.

In a first test, a case where all of the synapses were healthy (0% faulty) was considered. In this case, neurons #1 and #2 are activated by a presynaptic actuator and connected to the astrocyte via 2-AG signal. Fig. 6 shows the data related to variables of both neurons. The first and tenth synapses were selected as sample synapses to present data on PR values of synaptic transmission. Here, PR values of different synapses were seen to have similar properties. Synapses have an initial PR value of 0.8 that changes to an average value of 0.55 once the synapses get connected to DSE and e-SP. That is, astrocyte-neuron networks set the value of PR in steady state. Similar signals are observed for both neurons. The e-SP signal is identical for both neurons, as it is a global signal. Results of this simulation confirm that, in absence of any fault, the analog circuit is consistent with the software model [18].

In a second test, the circuit was investigated in the case when 20% of synapses were faulty, i.e. 2 of the 10 synapses related to neuron #2 had some fault injected into them so that the value of PR decreased. Fig. 7 indicates the results for both neurons. In this test, the first and second synapses for neuron #2 are damaged. Fig. 7(a) highlights in blue the value of PR for synaptic transmission for the damages synapse of neuron #2. After 400 μs, some error was injected into the first synapse of neuron #2, so that the value of PR changed to 0. As is evident in Fig. 7(b), the value of PR of the healthy synapse of neuron #2 (which is highlighted in blue) exceeds that of neuron #1 (which is marked in red), which indicates the repairing process. With increasing the value of PR, healthy synapses contribute to the maintenance of the performance of the circuit.

Table 3
The RMSE between MATLAB and HSPICE simulation.

Input frequency	RMSE Between q and V_q	RMSE Between p and V_p	Percent error q and V_q (%)	Percent error p and V_p (%)
10kHz	4.989 mV	6.654 mV	2.91	4.06
100kHz	4.576 mV	6.378 mV	2.30	3.47
1 MHz	4.343 mV	4.967 mV	1.75	2.53
10 MHz	4.124 mV	2.341 mV	1.20	1.35

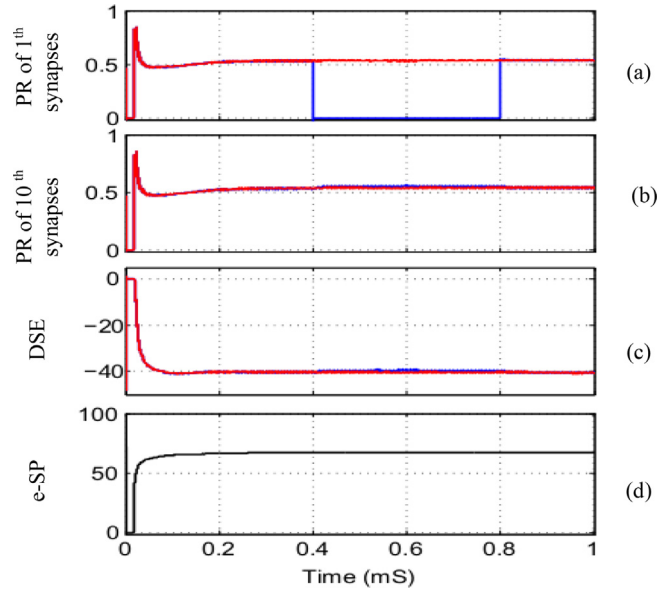

Fig. 7. Simulation results with 20% fault rate. (a) PR of the first synapses, (b) PR of the 10th synapses, (c) DSE signal of both neurons, (d) global e-SP signal. (red color) neuron #1, (blue color) neuron #2. (For interpretation of the references to color in this figure legend, the reader is referred to the web version of this article.)

In a third experiment, the associated rate of fault with neuron #2 was increased to 40% by making the synapses 1–4 of neuron #2 to be faulty. Fig. 8 demonstrates the simulation results. Following fault injection at 400 μs, PR of the first synapse is zero while that of the 10th synapse (i.e. healthy synapse) was increased by the astrocyte. The increase in PR at healthy synapses was greater on the network with the fault rate of 40%, as compared to that when the fault rate was set to 20%. It is seen in Fig. 7 (c) and (d) that, DSEs of the faulty synapses were somewhat reduced compared to that of healthy synapses (considering absolute values), which was pretty expected according to what was described above; however, similar e-SP was obtained for both neurons since

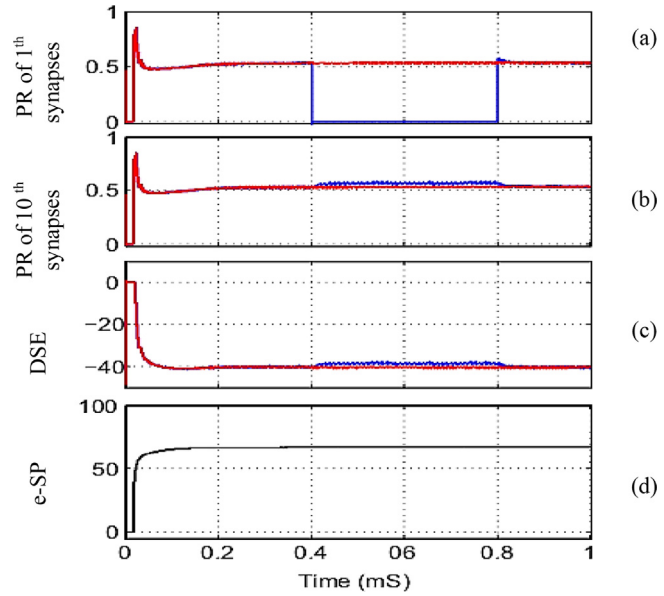

Fig. 8. Simulation results with 40% fault rate. (a) PR of the first synapses, (b) PR of the 10th synapse, (c) DSEs, (d) e-SP. (red color) neuron #1, (blue color) neuron #2. (For interpretation of the references to color in this figure legend, the reader is referred to the web version of this article.)

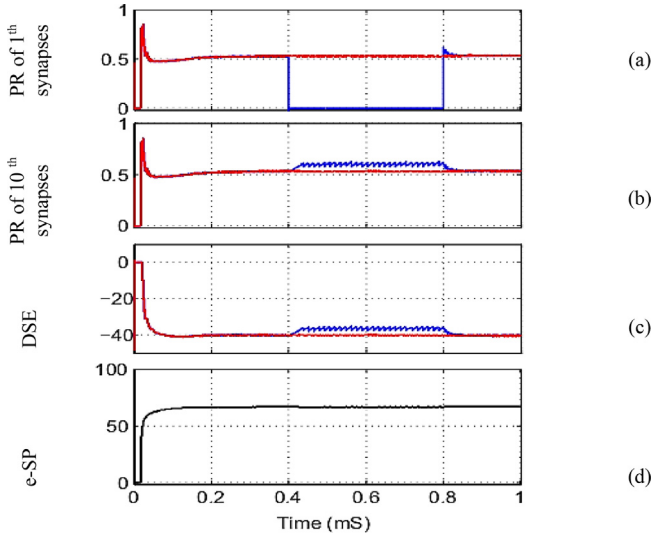

Fig. 9. Simulation results with 60% fault rate. (a) PR of the first synapses, (b) PR of the 10th synapse, (c) DSEs, (d) e-SP. (red color) neuron #1, (blue color) neuron #2. (For interpretation of the references to color in this figure legend, the reader is referred to the web version of this article.)

the signal is global. Considering the signals related to neuron #2, which were significantly faulty (e.g. at 40% in this test), this attenuated performance is acceptable since, according to the self-repairing principle, the system is capable of getting adapted to conditions and repairs itself.

In the fourth test, the proposed circuit was simulated with a fault rate of 60%, (i.e. 6 of the 10 synapses related to neuron #2 had some error injected into them,) with the simulation results demonstrated in Fig. 9. Based on this figure, it is observed that, following the occurrence of an error (i.e. at 400 μs), PR of the healthy synapse (e.g. 10th synapse) of neuron #2 gets closer to the initial PR value (0.8) to feedback from the astrocyte. The DSE of neuron #2 is decreased compared to neuron #1, which is an expected behavior defined in the evaluation of the software model [2]. Compared to previous cases, the value of e-SP, in this case, is slightly decreased, which is an expected behavior when considering the fault percentage.

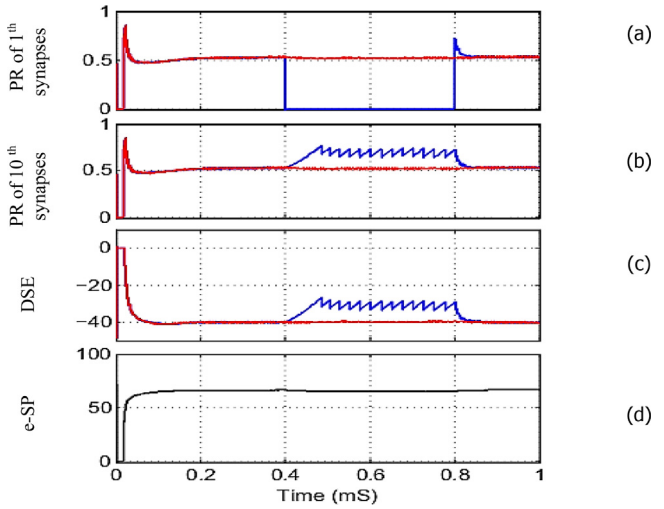

Fig. 10. Simulation results with 80% fault rate. (a) PR of first synapses, (b) PR of the 10th synapse, (c) DSEs, (d) e-SP. (red color) neuron #1, (blue color) neuron #2. (For interpretation of the references to color in this figure legend, the reader is referred to the web version of this article.)

In the fifth test, the proposed circuit was simulated with a fault rate of 80%, with the simulation results demonstrated in Fig. 10. In this figure, it is observed that, following the occurrence of faults (i.e. at 400 μs), PR of the healthy synapse (e.g. 10th synapse) of neuron #2 gets closer to the initial PR value (0.8) to feedback from the astrocyte. The DSE of neuron #2 is decreased compared to neuron #1, which is an expected behavior defined in the evaluation of the software model presented in [18]. Compared to previous cases, the value of e-SP, in this case, is just slightly decreased, which is an expected behavior when considering the fault percentage. As expected, all variables of neuron #1 remain constant and unchanged in all five figures, and the presence of a faulty synapses of neuron #2 imposes no impact on neuron #1.

According to the simulation results, it is observed that self-repairing capability can be implemented in analog circuits using the astrocyte circuit, while getting its good frequency adaptation. By providing indirect feedbacks (i.e. e-SP) and increasing PR of healthy synapses, astrocyte provides the circuit with the self-repairing capability and improves its performance.

5. Conclusion

Errors in neural networks cause incorrect results in the whole network. Recognizing this error and compensating for it greatly helps all neural networks to be able to continue working despite the error. Since astrocytes and synapses exhibit extensive activity in neural networks, they can assist the whole network in detecting and compensating for the occurred faults due to their capabilities. Self-repairing capability is among the principal components of a neural network. When a problem occurs in some fraction of local synapses, adjacent synapses are responsible for bearing the load resulting from the faulty synapses, mitigating network performance failure, so that the network can continue to serve normally. The astrocyte is a key element of self-repair, whose role in this property is already proven [16]. In this paper, an analog circuit was designed and presented to demonstrate the capability of astrocyte for self-repairing across local networks. By considering the changes in output astrocyte behavior at different frequencies, appropriate characteristics for self-repair can be found. As shown in this paper, when the input frequency of astrocyte increases (i.e. increase frequency of neighbor neurons), the astrocyte output signal has the continuous signal behavior. When the input frequency of astrocyte increases, the little change of input frequency cannot change the astrocyte output significantly. This property causes to keep constant approximately e-SP signal in low faults. This being constant signal causes to unchanged the e-SP signal, capturing the self-repairing capability by the proposed synapse circuit. We showed that the direct role of the astrocyte in the resultant synaptic fault percentages in self-repairing capability is significant. To the best of our knowledge, this is the first report on designing and presenting an astrocyte analog circuit for self-repairing in neural networks.

CRediT authorship contribution statement

Negin Veisi: Conceptualization, Methodology, Validation, Writing – original draft. **Gholamreza Karimi:** Investigation, Writing – review & editing, Data curation, Supervision. **Mahnaz Ranjbar:** Investigation, Data curation. **Derek Abbott:** Investigation, Writing – review & editing.

Declaration of Competing Interest

The authors declare that they have no known competing financial interests or personal relationships that could have appeared to influence the work reported in this paper.

References

[1] J. Liu, J. Harkin, L. Maguire, L. McDaid, J. Wade, M. McElholm, May). Self-repairing hardware with astrocyte-neuron networks, in: *2016 IEEE International Symposium on Circuits and Systems (ISCAS)*, 2016, pp. 1350–1353.

[2] J. Liu, L.J. Mcdaid, J. Harkin, S. Karim, A.P. Johnson, A.G. Millard, J. Hilder, D.M. Halliday, A.M. Tyrrell, J. Timmis, Exploring self-repair in a coupled spiking astrocyte neural network, IEEE Trans. Neural Networks Learn. Syst. 30 (3) (2019) 865–875.

[3] J. Liu, J. Harkin, L. McDaid, D.M. Halliday, A.M. Tyrrell, J. Timmis, July). Self-repairing mobile robotic car using astrocyte-neuron networks, in: *2016 International Joint Conference on Neural Networks (IJCNN)*, 2016, pp. 1379–1386.

[4] M. Ranjbar, M. Amiri, On the role of astrocyte analog circuit in neural frequency adaptation, Neural Comput. Appl. 28 (5) (2017) 1109–1121.

[5] G. Karimi, M. Ranjbar, M. Amirian, A. Shahim-aeen, A neuromorphic real-time VLSI design of Ca2+ dynamic in an astrocyte, Neurocomputing 272 (2018) 197–203.

[6] C. Bartolozzi, G. Indiveri, Synaptic dynamics in analog VLSI, Neural Comput. 19 (10) (2007) 2581–2603.

[7] M. Ranjbar, M. Amiri, Analog implementation of neuron–astrocyte interaction in tripartite synapse, J. Comput. Electron. 15 (1) (2016) 311–323.

[8] J.H. Wijekoon, P. Dudek, Integrated circuit implementation of a cortical neuron, in: 2008 IEEE International Symposium on Circuits and Systems, 2008, pp. 1784–1787.

[9] E.M. Izhikevich, Simple model of spiking neurons, IEEE Trans. Neural Networks 14 (6) (2003) 1569–1572.

[10] J.H. Wijekoon, P. Dudek, Simple analog VLSI circuit of a cortical neuron. In *2006 13th IEEE International Conference on Electronics, Circuits and Systems*, 2006, 1344–1347.

[11] J.H. Wijekoon, P. Dudek, Spiking and bursting firing patterns of a compact VLSI cortical neuron circuit. In *2007 International Joint Conference on Neural Networks*, 2007, 1332–1337.

[12] J.H.B. Wijekoon, P. Dudek, Compact silicon neuron circuit with spiking and bursting behaviour, Neural Networks 21 (2-3) (2008) 524–534.

[13] J. Liu, J. Harkin, L.P. Maguire, L.J. McDaid, J.J. Wade, SPANNER: a self-repairing spiking neural network hardware architecture, IEEE Trans. Neural Networks Learn. Syst. 29 (4) (2018) 1287–1300.

[14] J.J. Wade, L.J. McDaid, J. Harkin, V. Crunelli, J.S. Kelso, V. Beiu, Exploring retrograde signaling via astrocytes as a mechanism for self-repair, in: *The 2011 International Joint Conference on Neural Networks*, 2011, pp. 3149–3155.

[15] V. Volman, E. Ben-Jacob, H. Levine, The astrocyte as a gatekeeper of synaptic information transfer, Neural Comput. 19 (2) (2007) 303–326.

[16] M. Ranjbar, M. Amiri, An analog astrocyte–neuron interaction circuit for neuromorphic applications, J. Comput. Electron. 14 (3) (2015) 694–706.

[17] M. Naeem, L.J. McDaid, J. Harkin, J.J. Wade, J. Marsland, On the role of astroglial syncytia in self-repairing spiking neural networks, IEEE Trans. Neural Networks Learn. Syst. 26 (10) (2015) 2370–2380.

[18] J. Wade, L.J. McDaid, J. Harkin, V. Crunelli, S. Kelso, Self-repair in a bidirectionally coupled astrocyte-neuron (AN) system based on retrograde signaling, Front. Comput. Neurosci. 6 (2012) 76.

[19] X. Wei, C. Li, M. Lu, G. Yi, J. Wang, A novel astrocyte-mediated self-repairing CPG neural network, in: Chinese Control Conference, IEEE, 2019, pp. 4872–4877.

[20] J. Yang, D.C. Keezer (2019, November). (2019) A Framework for Design of Self-Repairing Digital Systems. In *2019 IEEE International Test Conference (ITC)*. 1–10.

[21] B.E. Alger, Retrograde signaling in the regulation of synaptic transmission: focus on endocannabinoids, Prog. Neurobiol. 68 (4) (2002) 247–286.

[22] M. Navarrete, A. Araque, Endocannabinoids potentiate synaptic transmission through stimulation of astrocytes, Neuron 68 (1) (2010) 113–126.

[23] Y.-X. Li, J. Rinzel, Equations for InsP3 receptor-mediated [Ca2+] i oscillations derived from a detailed kinetic model: a Hodgkin-Huxley like formalism, J. Theor. Biol. 166 (4) (1994) 461–473.

[24] W. Gerstner, W.M. Kistler, Spiking Neuron Models: Single Neurons, Populations, Plasticity, Cambridge University Press, 2002.

[25] P. Kurosinski, J. Götz, Glial cells under physiologic and pathologic conditions, Arch. Neurol. 59 (10) (2002) 1524–1528.

[26] G. Montaseri, M.J. Yazdanpanah, M. Amiri, Astrocyte-inspired controller design for desynchronization of two coupled limit-cycle oscillators, in: *2011 third world congress on nature and biologically inspired computing*, 2011, pp. 195–200.

Negin Veisi was born in Kordestan, Iran in 1992. She received the B.Sc. degree in electronic engineering and M.Sc. degree in micro and Nano electronic engineering from Razi University, Kermanshah, Iran in 2014 and 2018, respectively. Her current research interests include analog electronic circuit design, and neuromorphic circuits.

Gholamreza Karimi was born in Kermanshah, Iran in 1978. He received the B.S. and M.S. and PhD degrees in electrical engineering from Iran University of Science and Technology (IUST) in 1999, 2001 and 2006 respectively. He is currently a Full Professor in Electrical Department at Razi University, Kermanshah. His research interests include low power Analog and Digital IC design, RF IC design, Neuromorphic VLSI, and microwave devices.

Mahnaz Ranjbar was born in Hamedan, Iran in 1988. She received the B.Sc in Electronics Engineering from Islamic Azad University, Kermanshah, 2010 and the MSc degree in Electronics Engineering from Islamic Azad University, Central Tehran Branch Iran in 2012. Her current research is in analog integrated circuit, fuzzy systems, RF filters, and neural networks.

D. Abbott was born in South Kensington, London, U.K. He received the B.Sc. (honors) degree in physics from Loughborough University, Leicestershire, U.K., in 1982 and the Ph.D. degree in electrical and electronic engineering from The University of Adelaide, Adelaide, S.A. Australia, in 1995, under K. Eshraghian and B.R. Davis. From 1978 to 1986, he was a Research Engineer at the GEC Hirst Research Centre, London, U.K. From 1986 to 1987, he was a VLSI Design Engineer at Austek Microsystems, Australia. Since 1987, he has been with The University of Adelaide, where he is presently a full Professor with the School of Electrical and Electronic Engineering. He coedited Quantum Aspects of Life (London, U.K.: Imperial College Press, 2008), coauthored Stochastic Resonance (Cambridge, U.K.: Cambridge University Press, 2012), and coauthored Terahertz Imaging for Biomedical Applications (New York, NY, USA: Springer-Verlag, 2012). He holds over 800 publications/patents and has been an invited speaker at over 100 institutions. His interests are in the area of multidisciplinary physics and electronic engineering applied to complex systems. His research programs span a number of areas of stochastics, game theory, photonics, biomedical engineering, and computational neuroscience. He is a Fellow of the Institute of Physics (IOP) and a Fellow of the IEEE. He has won a number of awards including the South Australian Tall Poppy Award for Science (2004), the Premier's SA Great Award in Science and Technology for outstanding contributions to South Australia (2004), and an Australian Research Council (ARC) Future Fellowship (2012). With his colleagues, he won an IEEE Sensors Journal best paper award (2014). He has served as an Editor and/or Guest Editor for a number of journals including the IEEE Journal of Solid-State Circuits, Journal of Optics B, the Microelectronics Journal, Chaos, Smart Structures and Materials, Fluctuation and Noise Letters, and is currently on the editorial boards of the Proceedings of the IEEE, the IEEE Photonics Journal, and Nature's Scientific Reports.